STEM CELLS AND DEVELOPMENT
Volume 24, Number 6, 2015

DOI: 10.1089/scd.2014.0209

Transient Receptor Potential Channels and Their Role in Modulating Radial Glial–Neuronal Interaction: A Signaling Pathway Involving mGluR5

Lauri M. Louhivuori, Linda Jansson, Pauli M. Turunen, Maria H. Jäntti, Tommy Nordström, Verna Louhivuori, and Karl E. Åkerman

The guidance of developing neurons to the right position in the central nervous system is of central importance in brain development. Canonical transient receptor potential (TRPC) channels are thought to mediate turning responses of growth cones to guidance cues through fine control of calcium transients. Proliferating and 1- to 5-day-differentiated neural progenitor cells (NPCs) showed expression of *Trpc1* and *Trpc3* mRNA, while *Trpc4–7* was not clearly detected. Time-lapse imaging showed that the motility pattern of neuronal cells was phasic with bursts of rapid movement ($>60\,\mu m/h$), changes in direction, and intermittent slow phases or stallings ($<40\,\mu m/h$), which frequently occurred in close contact with radial glial processes. Genetic interference with the TRPC3 and TRPC1 channel enhanced the motility of NPCs (burst frequency/stalling frequency). TRPC3-deficient cells or cells treated with the TRPC3 blocker pyr3 infrequently changed direction and seldom contacted radial glial processes. TRPC channels are also activated by group I metabotropic glutamate receptors (mGluR1 and mGluR5). As shown here, pyr3 blocked the calcium response mediated through mGluR5 in radial glial processes. Furthermore, 2-methyl-6-(phenylethynyl)pyridine, a blocker of mGluR5, affected the motility pattern in a similar way as TRPC3/6 double knockout or pyr3. The results suggest that radial glial cells exert attractant signals to migrating neuronal cells, which alter their motility pattern. Our results suggest that mGluR5 acting through TRPC3 is of central importance in radial glial-mediated neuronal guidance.

Introduction

Neuronal motility is a fundamental feature that underlies the development, regeneration, and plasticity of the nervous system and is essential for normal neocortical function. The radial unit hypothesis provides a theoretical framework whereby neurons migrate along a path established by parallel radial glial fibers [1]. Guiding by external cues ensures that specific neurons come to reside in specific layers of the neocortex.

Accumulating evidence indicates that changes in the cytosolic calcium concentrations play important and diverse roles in the migratory process, including responses to cues and regulation of molecular motors involved in motility. In this context, recent evidence suggests that nonselective cation channels of the canonical transient receptor potential (TRPC) channels family mediate responses to chemoattractant and repellant factors. Two normally chemoattractive factors—netrin and brain-derived neurotrophic factor (BDNF)—are believed to increase calcium concentrations in neurons by triggering influx of the ion and its release from intracellular stores. Interference with TRPC1 inhibits netrin-induced turning of growth axons [2,3], and RNAi against *Trpc3* interferes with BDNF-induced turning of axons [4].

A link between TRPC channels and the nonselective cation current activated by BDNF has been shown in several studies. TRPC3 and the tyrosine kinase B (TrkB), a BDNF receptor, were shown to colocalize in several neuronal populations and were coimmunoprecipitated. TRPC3 was shown to contribute to the BDNF current [5,6]. BDNF causes Ca^{2+} elevations also in a subpopulation of migrating progenitors expressing TrkB receptors [7]. Considering the high expression of *Trpc3* mRNA and TRPC channel proteins in specific regions of the brain [4,8] along with particularly high expression in embryonic tissues [9], one might speculate about the function of TRPC3 in the development of neuronal tissue. The role of TRPCs in embryonic corticogenesis is, however, limited. Calcium entry through TRPC1 channel activation appears to play a critical role in basic fibroblast growth factor-induced neural stem cell proliferation [10]. TRPC1 and TRPC4 have been reported to regulate neurite extension in human embryonic stem

Biomedicum Helsinki, Institute of Biomedicine/Physiology, University of Helsinki, Helsinki, Finland.

cell-derived neurons [11]. A TRPC1-mediated increase in calcium entry has been shown to be required for the proliferation of adult hippocampal neural progenitor cells (NPCs) [12] as well as mediating a role in the proliferation of oligodendrocyte progenitor cells [13].

In addition to typical chemoattractant factors, also group I metabotropic glutamate receptors (mGluR1 and mGluR5) couple to activate members of the TRPC channel family in neurons [14,15]. They are involved in activity-dependent forms of synaptic plasticity, both during development and in the adult life. The mGluR5 glutamate receptor is involved in neurogenesis [16–19] and appears to be expressed almost exclusively in radial glia in vitro migrating neurosphere-derived cells [20]. The similarity of the signaling mechanism involving mGluR5 and TrkB receptors might suggest that the developmental responses mediated through these receptors may also involve TRPC channels. Blocking of mGluR5 receptors significantly alters the motility pattern of migrating NPCs [20] and the mGluR5 calcium response displayed sensitivity to the TRPC3 blocker pyr3.

So far, information concerning neurogenesis and brain development from gene-deficient animal models is limited. The aim of this study was to elucidate the role of TRPC channels in the early stages of NPC differentiation with a particular emphasis on TRPC3, using the neurosphere assay to investigate neuronal migration in embryonic mice lacking functional TRPC channels.

Materials and Methods

Mice

All animals were housed in standard laboratory conditions in qualified animal facilities in accordance with the National Institutes of Health guidelines. Two different inbred strains of mice Friends virus B (FVB) and 129SvJ/C57Bl6/N (C57) were used in this study. We have extensively characterized the neural progenitor calcium responses from FVB mice in previous studies [7,21–23], and thus, our initial characterizations in this study were done with this strain. Our interest in elucidating the function of TRPC channels in neural progenitor migration as well as the current lack of specific channel blockers for the TRPCs led us to use TRPC-deficient C57 mice. TRPC1/TRPC4/TRPC5-deficient mice (1/4/5 TKO) [24] and TRPC3/TRPC6-deficient mice (3/6 DKO) have been described [25]. All TRPC-deficient mice were from a mixed C57 genetic background. F1 offspring of C57 matings were used as controls. Our mRNA and calcium experiments showed no marked differences in responses between the wild-type C57 controls and FVB controls.

Cell culture and neuronal differentiation

NPCs were isolated from the walls of the lateral ventricles of embryonic day 14 FVB mice and TRPC-deficient mice (3/6 DKO and 1/4/5 TKO mice) and their respective wild-type controls, as described previously [26]. Briefly, cells were grown as free-floating aggregates, known as neurospheres, in Dulbecco's Modified Eagle's Medium:Ham's Nutrient Mixture F-12 media (1:1) containing B27 supplement (both from Gibco, Life Technologies Ltd.), 2 mM L-glutamine, 15 mM 4-(2-hydroxyethyl)piperazine-1-ethanesulfonic acid (HEPES), 100 U/mL penicillin, and 100 U/mL streptomycin (all from Sigma-Aldrich), in the presence of 10 ng/mL fibroblast growth factor and 20 ng/mL epidermal growth factor (both from PeproTech EC Ltd.), in a 5% CO_2 humidified incubator at 37°C. The culture media were refreshed twice a week and growth factors were added thrice a week. Cells were passaged by manual trituration at approximately 7- to 10-day intervals. The maximum number of NPC passages was 15. For neuronal differentiation, neurospheres were plated on poly-DL-ornithine (Sigma-Aldrich)-coated culture dishes or cover glasses in the absence of mitogens. Growth factor withdrawal induced spontaneous neuronal differentiation.

Calcium imaging

Calcium imaging was performed as described previously [22,23,26]. For the experiments, 20–30 neurospheres were plated on poly-DL-ornithine-coated 25-mm cover glasses and differentiated for the indicated time periods. The cells were then incubated with 4 μM fura-2 acetoxymethyl ester (Molecular Probes Invitrogen, Life Technologies Ltd.) dissolved in dimethyl sulfoxide (Sigma-Aldrich) at 37°C for 20 min in HEPES-buffered media (pH 7.4) consisting of 137 mM NaCl, 5 mM KCl, 0.44 mM KH_2PO_4, 4.2 mM $NaHCO_3$, 2 mM $CaCl_2$, 0.5 mM $MgCl_2$, 10 mM HEPES, and 10 mM glucose (all from Sigma), before imaging. After incubation, cover glasses were attached to a temperated perfusion chamber on the microscope (Nikon; TMS inverted microscope, 20× objective) and perfused at 2 mL/min at 37°C. Using 340 and 380 nm light excitation filter changer under the control of the InCytIM-2 System (Intracellular Imaging, Inc.) and a dichroic mirror (DM430; Nikon), up to 100 cells could be recorded simultaneously. Cells derived from one neurosphere were imaged in each experiment. Light emission was measured through a 510-nm barrier filter with an integrating charge-coupled device camera (COHU, Inc.). A ratioed (340 nm/380 nm) image was acquired each second. The data collected were analyzed with the InCyt 4.5 software (Intracellular Imaging, Inc.) and further processed with the Origin 6.0 software (OriginLabCorp).

RNA isolation, cDNA synthesis, and real-time PCR

Total RNA was isolated from proliferating NPCs and NPCs differentiated for 1, 3, or 5 days using the RNeasy Mini Kit (Qiagen) according to the manufacturer's instructions. The *Trpc* primers used (Table 1; *Trpc*-3, -6, -7 from Elg et al. [27]). RNA was quantified using a NanoDrop ND8000 spectrophotometer (Thermo Scientific) and the Transcriptor High Fidelity cDNA Synthesis Kit (Roche Applied Science), and random hexamer primers were used for cDNA synthesis. cDNA was amplified with the LightCycler® 480 SYBR Green I Master Kit and LightCycler® 480 system (both from Roche Applied Science). The PCR data were normalized to *GAPDH* and *β-actin* or *18S rRNA* using geNorm software.

Immunocytochemistry

Differentiating cells were fixed and immunostained as described previously [23]. Primary antibodies used were the mouse monoclonal anti-microtubule-associated protein (MAP)-2 (MAB364; Millipore) and the rabbit polyclonal

Table 1. Primers for Quantitative Real-Time Polymerase Chain Reaction

Target	*Forward primers (5′–3′)*	*Reverse primers (5′–3′)*	*Product size (bp)*
Trpc1	TTGCTGGCGTGCGACAAGGG	GTGCATCTGCGGACTGACAACCG	187
Trpc3	GGAGAGCGATCTGAGCGAAGT	GGGAGCCATTTGTCTCTAGCA	75
Trpc4	TGTAGGCGATGCGCTGCTTCA	GAATGGGAGGCACCTGCTTCTCTC	107
Trpc5	GCCATCCGCAAGGAGGTGGTAG	CATCATCAGCGTGGGAACCTGCT	90
Trpc6	ACTACATTGGCGCAAAACAGAA	AGAAAGACCAAAGATAGCCCAGAA	86
Trpc7	TCCATAGGCCTCCCTTTTCTC	TCCTCAGGGTTTGTCCTAGCTT	73
β-actin	GTGGATCAGCAAGCAGGAGT	GAAAGGGTGTAAAACGCAGC	99
GAPDH	AACGACCCCTTCATTGAC	TCCACGACATACTCAGCAC	191
18S rRNA	AAACGGCTACCACATCCAAG	GAAAGCTCCGGGACATTAAC	112

TRPC, canonical transient receptor potential channels.

anti-excitatory amino acid transporter 1, also known as glial glutamate-aspartate transporter (GLAST, ab416; Abcam). Secondary antibodies used were Alexa Fluor 488® goat anti-rabbit immunoglobulin G (IgG, A11008) and Alexa Fluor 568® goat anti-mouse IgG (A11004, both from Molecular Probes Invitrogen, Life Technologies Ltd). Vectashield mounting media containing 4′,6-diaminodino-2-phenylindole (DAPI) were used for nuclear staining (Vector Laboratories, Inc.) and viewed and photographed using an Olympus AX70 Provis microscope (Olympus), equipped with fluorescence optics and a charge-coupled device camera (PCO AG).

Time-lapse imaging

Time-lapse imaging of cellular movement was performed in a self-contained cell-culturing instrument combining phase-contrast microscopy, automation, and environmental control (Cell-IQ® system; Chip-Man Technologies Ltd.). The imaging system enables continuous monitoring of adherent cells in two plates in an integrated plate holder. Time-lapse images were analyzed with ImageJ and its plugin MJtracker and the data quantified with Excel (Microscoft) and Origin 6.0 (OriginLabCorp). The motility index of the cells was defined as the number of time points the cell moved with a speed higher than 40 μm/h divided by the number of time points the speed of the cell was below this value at a time period of at least 10 h. An additional logarithmic linear transformation was performed to the data points.

Data analysis

Statistical significance between groups was determined using Student's nonpaired *t*-test. Significances are as follows: $P > 0.05$ not significant (ns), $^{*}P < 0.05$, $^{**}P < 0.01$, $^{***}P < 0.001$.

Results

mRNA expression of trpc channels in proliferating and differentiating NPCs

Removal of mitogen leads to a migration of neuroblasts and radial glial processes from the neurosphere. We tested for the expression of the *Trpc* in proliferating and 1 and 3 days differentiated NPCs propagated from E14 mice. All the *Trpc* mRNAs were detected with the primers we used (Table 1) in the whole brain cDNA preparation of juvenile mice. The mRNA for *Trpc1* and *Trpc3* was detected from E14 NPCs at proliferating and 1 and 3 days differentiated time periods in cells from C57 mice (Fig. 1A). A weak signal was occasionally seen for *Trpc4* and 5 mRNA (data not shown). No mRNA was detected for *Trpc6* and 7 (Fig. 1A). The expression pattern was similar in cells from the FVB mice strain (data not shown) used in previous studies [20,26]. Using RT-qPCR (normalized against proliferating cells), the mRNA expression for *Trpc1* and *Trpc3* was analyzed in cells from 3/6 DKO and 1/4/5 TKO mice. There was no significant change in the mRNA levels for *Trpc1* in 3/6 DKO cells and *Trpc3* in 1/4/5 TKO cells (Supplementary Fig. S1A, B; Supplementary Data are available online at www.liebertpub.com/scd).

Responses of migrating neurosphere-derived cells to diacylglycerol

We directed our attention to the TRPC3 and TRPC1 channels due to their abundance in the early stages of differentiation. To test the functionality of TRPC3 channels, we challenged NPCs with a diacylglycerol analogue dioctanoyl glycerol (DOG, 30 μM). The response of the migrating cells to the ligand was monitored using calcium imaging. Since DOG might be metabolized by the cells and DOG stimulation activates protein kinase C, which has been shown to inhibit TRPC3 channels, the cells were challenged with DOG together with a diacylglycerol kinase inhibitor R59949 to block metabolism of DOG and GF109203X a blocker of protein kinase C isoforms. Kainate (50 μM) was used to test the viability of the cells. R59949 and GF109203X had no effect on intracellular Ca^{2+} in the absence of DOG (data not shown).

In the presence of 1 μM pyr3, only a small response to DOG was obtained (Fig. 1B, E) in cells from the FVB strain. A robust response was obtained in the same cells after pyr3 had been washed away.

In view of these results, we cultured cells from knockout mice devoid of functional TRPC3 channels and stimulated with DOG. As shown in Fig. 1C, wild-type cells with the genetic C57 background responded to DOG (in the presence of R59949 and GF109203X) in a similar way as FVB mice. Cells devoid of functional TRPC3/6 channels were resistant to the challenge with DOG yet responded to kainate (Fig. 1D, F), while cells devoid of functional TRPC1/4/5 still responded to DOG (Fig. 1F) although the average magnitude appeared less. A response was obtained in 37 ± 20% of the wild-type (WT) cells ($N = 7$ measurements with 50 cells

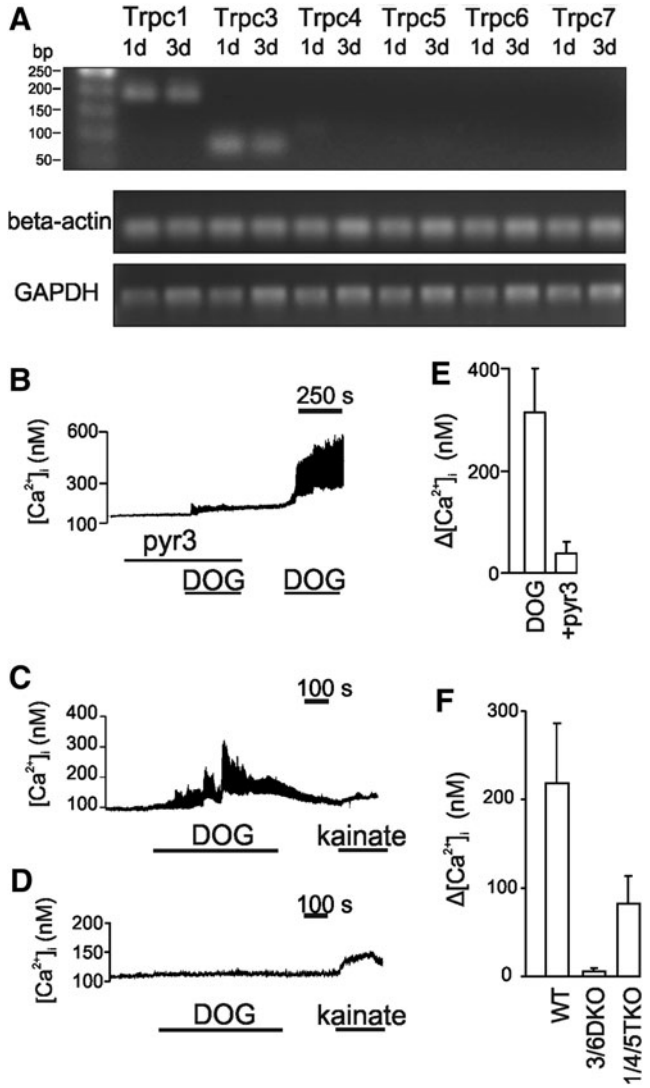

FIG. 1. Canonical transient receptor potential (*Trpc*) channels mRNA expression in neural progenitor cells. **(A)** Cells were differentiated for different time periods. Aliquots of each PCR amplified DNA were loaded on 1.5% agarose gel and poststained with SYBRgreenI. Bands (*upper panel*) were visualized by UV transillumination. **(B)** Effect of dioctanoyl glycerol on intracellular Ca^{2+} in migrating neural progenitor cells. Cells were differentiated for 4 days. An average trace of all recorded cells (21) responding to dioctanoyl glycerol (DOG) ± standard error of the mean (SEM). Friends virus B (FVB) cells were treated with 1 μM pyr3 and 30 μM DOG, where indicated. In **(C)**, an average trace of all recorded wild-type C57 cells ($n = 18$) responding to 30 μM DOG and 50 μM kainate ± SEM. **(D)** Average of all TRPC3/TRPC6-deficient mice (3/6 DKO) cells in the field of vision ($n = 40$). None of the cells responded to DOG, yet still responded to 50 μM kainate. **(E)** Statistics for experiments similar to **(B)** for FVB mice. ($N = 5$, 35–50 cells per experiment). **(F)** Statistics for experiments similar to **(B)** for wild-type C57, 3/6 DKO, and TRPC1/TRPC4/TRPC5-deficient (1/4/5 TKO) mice ($N = 7$ for C57, $N = 8$ for 3/6 DKO cells, and $N = 5$ for 1/4/5 TKO cells ± SEM, 35–50 cells per experiment).

analyzed from each experiment) and in 29 ± 10% of the cells from 1/4/5 TKO ($N = 5$).

NPC migration

Due to the potential role of TRP channels as chemosensors and reported guidance mediators of extracellular cues [28], we proceeded to analyze the role of TRPC channels on NPC migration. To visualize the migratory behavior of NPCs, time-lapse microscopy was used to document the behavior of these NPCs as they migrated from the neurosphere.

Neuronal cells moving outside the radial layer were analyzed for their motility pattern. It was observed that these NPCs routinely changed directions while migrating, alternating between pauses and bursts. These observations are consistent with previously described subventricular zone neurons migrating in slices [29–31]. Examples of the movement of individual control cells (Fig. 2A, B) and cells treated with 1 μM pyr3 are shown in Fig. 2C and D. As shown previously [20,23], neuron-like cells exiting from the radial glial layer move in a phasic manner with fast bursts of rapid movement and intermittent stationary phases. During burst, the cells usually have a typical bipolar shape (Fig. 2A, see inset) with a thicker leading process followed by a longer and thinner process lagging behind. The stationary phases or stallings are depicted by arrows in the control trace in Fig. 2A. During stalling phases, the cells are not totally stationary, but move slowly in several directions (speed below 40 μm/h; depicted by dotted line). Note the extension of multiple processes during the stationary phase (Fig. 2A, inset).

The spatial distribution of the cell at the different time points shows that during stalling (Fig. 2A, arrows), it frequently changes its direction of movement (Fig. 2B). The movement of a 1 μM pyr3-treated cell is shown in Fig. 2C. Note the long burst of movement with short periods of stalling (speed below 40 μm/h; depicted by dotted line). The spatial distribution of this cell is also different from the control. It does not undergo any abrupt changes in direction (Fig. 2D). Statistics from similar measurements from 51 control cells and 42 pyr3-treated cells is shown in Fig. 2E–H.

Due to the phasic motility pattern with intermittent bursts of movement with a speed > 60 μm/h and stalling < 40 μm/h, the average speed of movement may not be an appropriate parameter for analyzing cellular motility [23]. The motility index of the cells was therefore defined as the number of time points the cell moved with a speed higher than 40 μm/h divided by the number of time points the speed of the cell was below this value at a time period of at least 10 h. The cutoff speed of 40 μm/h was chosen since the cells seldom move forward below this value for longer periods and during stalling, the speed was < 40 μm/h. Some cells moved with a low speed without bursts of rapid movement or stopped moving altogether during the period of analysis. To exclude these cells from the statistics, a further criterion was that the cells analyzed had to move at least twice with a speed of 60 μm/h during a 10-h period.

The average motility index of control cells in different experiments is usually between 1 and 2 (data from over 1,000 cells). The average motility index was significantly higher in the pyr3-treated cells (Fig. 2E; linear transformation

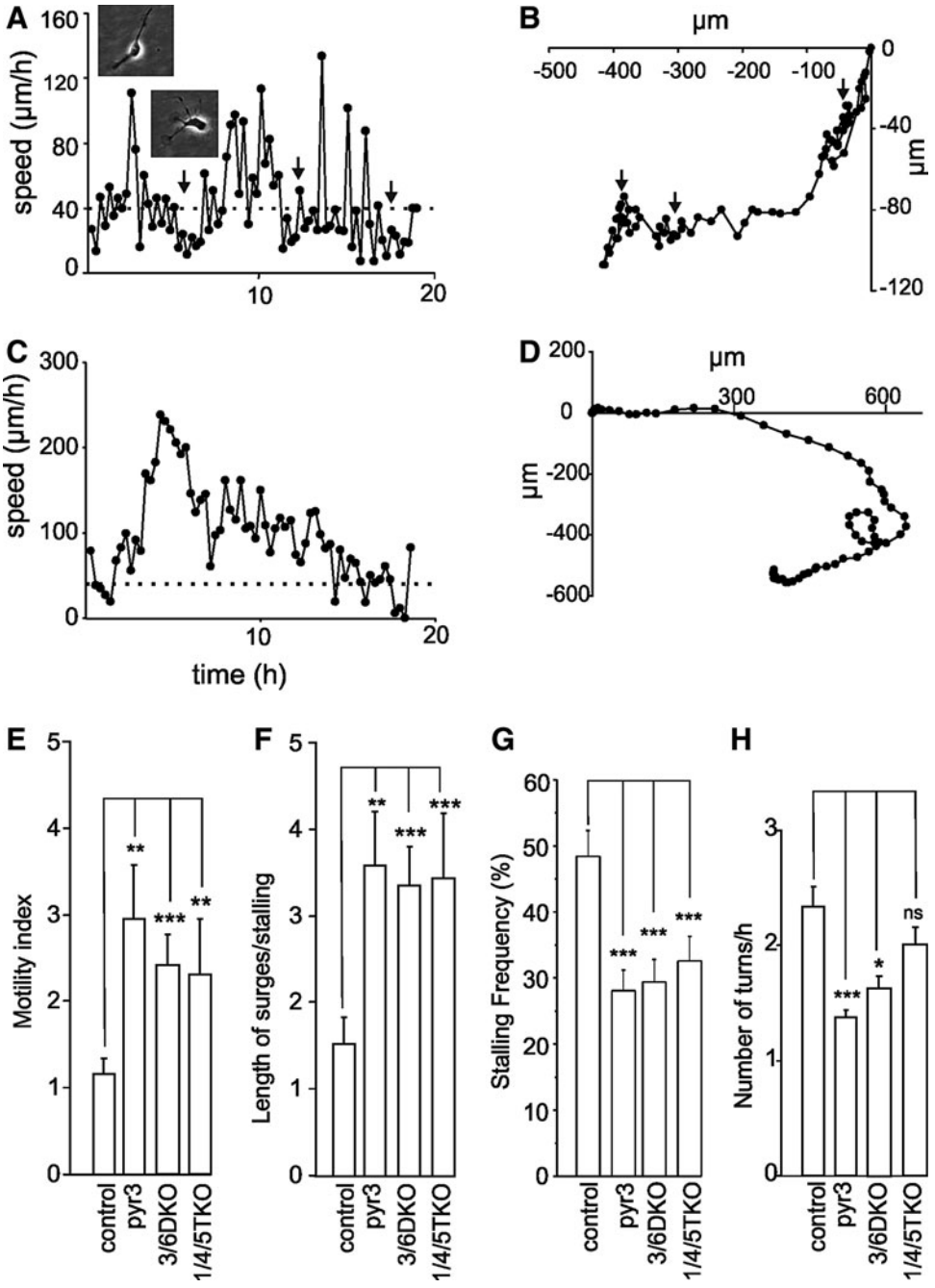

FIG. 2. Role of TRPC channels in motility pattern of migrating cells. Images were taken every 15 min. The rate and path of a single freely moving as a function of time was tracked. **(A)** Speed versus time in a control cell. *Inserts* showing the morphology of the cell tracked at different phases. **(B)** Graph of the path of cell movement (*X* coordinates plotted against *Y* coordinates). **(C, D)** A cell treated with 1 μM pyr3. **(E–H)** All cells moving with a speed above 60 μm/h twice or more during a period 10 h or more were analyzed statistically. **(E)** Motility coefficient (number time points with a speed above 40 μm/h divided by time points below 40 μm/h) for control (10 recordings 51 cells), pyr3-treated cells (eight recordings 42 cells), cells from 3/6 DKO (12 recordings 49 cells), and 1/4/5 TKO mice (19 recordings 64 cells). **(F)** Length of high motility phases (>40 μm/h) divided by length of phases with low motility (<40 μm/h) for control, pyr3-treated cells, cells from 3/6 DKO, and 1/4/5 TKO mice. **(G)** Frequency and duration of stalling periods (<40 μm/h) as a percentage of total time points for controls (10 recordings, 51 cells), pyr3-treated cells (eight recordings, 12 cells), cells from 3/6 DKO (12 recordings, 49 cells), and 1/4/5 TKO mice (19 recordings, 64 cells). **(H)** The number of times each cell changes direction as seen in either the *X* or *Y* coordinates during a time period of ≥ 10 h was counted for control, pyr3-treated cells, cells from 3/6 DKO, and 1/4/5TKO mice. ns, not significant; $*P<0.05$; $**P<0.01$; $***P<0.001$.

Table 2. Linear Transformation Statistics for Figure 2E

	Mean	± *SEM*	*Significance* ($p < 0.05$)	*Probability* (*p value*)
Controls	1.02	0.04	—	—
Pyr3	1.44	0.06	Yes	0.002
3/6 DKO	1.55	0.09	Yes	6.3×10^{-7}
1/4/5 TKO	1.37	0.04	Yes	0.001

SEM, standard error of the means; 1/4/5 TKO, TRPC1/TRPC4/TRPC5-deficient mice; 3/6 DKO, TRPC3/TRPC6-deficient mice.

values Table 2). A similar result was obtained if the average length of bursts of motion for each cell was divided by the average length of stalling (Fig. 2F). The motility index of the 3/6 DKO and 1/4/5 TKO cells analyzed as described above was also significantly higher compared to cells from wild-type littermates (Fig. 2E, F). This was also reflected as a reduction in the frequency stalling periods. The 1/4/5 TKO cells showed less stalling than the pyr3-treated and 3/6 DKO cells (Fig. 2G). As seen in Fig. 2B, the cells made sudden shifts in their direction of movement. Since slowing down and turning may be due to chemotactic influences, we counted the frequency by which the cells change direction. The pyr3-treated and 3/6 DKO cells also showed significantly less changes of direction (Fig. 2H). The turning frequency of the 1/4/5 TKO cells did not significantly differ from the controls (Fig. 2H).

BDNF, a neurotrophin, which stimulates cell migration and acts as a chemoattractant [32], also causes an increased motility index of the neuron-like cells [20]. In neurons, some of the effects of BDNF are mediated through activation of TRPC3 channels [5,6]. It was therefore of interest to see whether the effect on the motility index is mediated by TRPC3. BDNF did not affect the motility of the 3/6 DKO cells (Fig. 3; linear transformation values Table 3). Interestingly, BDNF further potentiated the mobility index of the 1/4/5 TKO cells. There was a large variability in the motility index and turning frequency of different cells. To study a possible correlation between these parameters, we plotted the motility against the turning frequency for each cell. There was no apparent correlation between the two parameters (Supplementary Fig. S2A) also seen as the very large standard deviation in Supplementary Fig. S2B. BDNF-treated and 1/4/5 TKO cells showed an increase in motility with no significant change in the turning frequency, while in pyr3-treated cells and 3/6 DKO cells, a significant decrease in turning frequency was seen.

The bias of pyr3-treated cells and 3/6 DKO cells toward a lower turning frequency is reminiscent of our previous finding with 2-methyl-6-(phenylethynyl)pyridine (MPEP), a blocker of mGluR5 receptors [20]. Data from MPEP-treated cells are included in Supplementary Fig. S2B for comparison. MPEP increased the motility index and reduced the turning frequency in a similar way as pyr3. Since the mGluR5 blocker MPEP had an effect reminiscent of pyr3 (and 3/6 DKO) and the action of mGluR5, based on calcium imaging and immunocytochemistry, is mainly seen in radial glia [20], one possibility would be that radial processes influence neuronal motility.

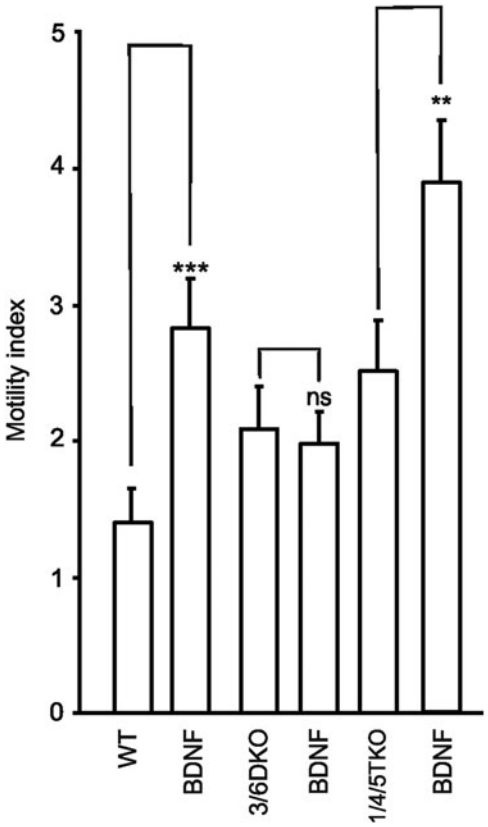

FIG. 3. The effect of 10 ng/mL brain-derived neurotrophic factor (BDNF) on the motility pattern in wild-type and 3/6 DKO mice. Wild type (12 experiments, 78 cells), BDNF (eight experiments, 39 cells), 3/6 DKO, BDNF/3/6 DKO (six recordings, 34 cells), 1/4/5 TKO (six recordings, 37 cells), and BDNF/1/4/5 TKO (nine recordings, 49 cells). ns, not significant; $^{**}P < 0.01$; $^{***}P < 0.001$.

mGluR5-stimulated calcium responses display pyr3 sensitivity

Group I metabotropic glutamate receptors (mGluR1 and mGluR5) have been shown to activate members of the TRPC channel family [14,15]. We challenged migrating NPCs with 3,5-dihydroxyphenylglycine (DHPG), an agonist of these receptors. A low concentration of DHPG (10 μM) causes a rise in intracellular calcium, which is dependent on extracellular calcium [23], and activates a nonselective cation current, while higher concentrations cause a massive release of calcium from internal stores [33]. The response to

Table 3. Linear Transformation Statistics for Figure 3

	Mean	± *SEM*	*Significance* ($p < 0.05$)	*Probability* (*p value*)
Controls	1.08	0.04	—	—
Controls + BDNF	1.43	0.05	Yes	6.4×10^{-4}
3/6 DKO	1.39	0.09	—	—
3/6 DKO + BDNF	1.32	0.06	No	0.98
1/4/5 TKO	1.32	0.04	—	—
1/4/5 TKO + BDNF	1.58	0.05	Yes	0.007

BDNF, brain-derived neurotrophic factor.

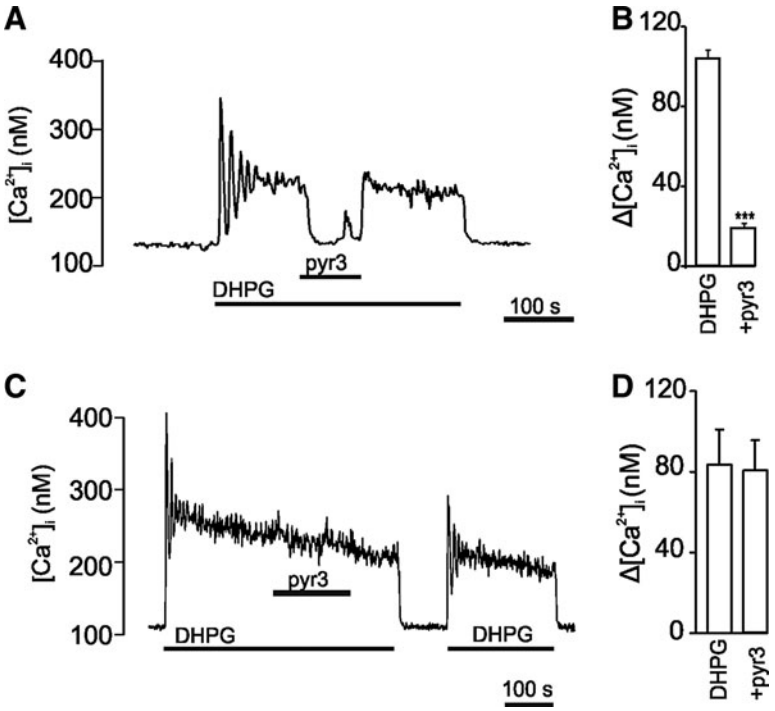

FIG. 4. Effect of 3,5-dihydroxyphenylglycine (DHPG) and pyr3 in wild-type (WT) C57 and 3/6 DKO cells. Recordings of intracellular Ca^{2+} with fura-2 in individual cells. **(A)** WT cells were challenged with 10 μM DHPG and 1 μM pyr3, where indicated. **(B)** Statistics for WT cells ($N = 6$ experiments with 35–50 cells in each measurement). The data were quantified by taking an average of 4–5 readings before and after the addition of pyr3. **(C)** 3/6 DKO cells were challenged with 10 μM DHPG and 1 μM pyr3, where indicated. **(D)** Statistics for 3/6 DKO cells ($N = 6$ experiments with 35–50 cells in each measurement). Average ± standard deviation (SD). $***P < 0.001$.

DHPG was reversed by application of 1 μM pyr3 in cells with the C57 genetic background (Fig. 4A, B). The cells from the 3/6 DKO mice responded to DHPG to about the same extent as wild-type cells, but they were resistant to pyr3 (Fig. 4C, D). Using a higher concentration of pyr3 (10 μM) caused an increase in calcium in some cells and had an inhibitory effect also in 3/6 DKO cells (data not shown).

TRPC3/6 DKO disturbs the structure of radial glial processes

The apparent absence of mGluR5 from the outer neuronal cells [20,23] whose motility pattern was monitored as well as the sensitivity of the mGluR5 response to pyr3 would suggest that the radial glial cells somehow influence the motility of neuronal cells by means of mGluR5 acting through TRPC3. Our previous studies have shown a cellular phenotype distribution with regard to the distance from the mothersphere [20,23,26]. The neuronal marker MAP-2 dominates at the outer regions, while the radial glial marker GLAST dominates close to the neurosphere as a dense network. Our motility index data suggest a radial glial influence on neuronal migration. We therefore proceeded to investigate whether any gross morphological differences could be observed in the radial glial network between the TRPC knockouts compared to wild types.

Cells were immunocytochemically costained with antibodies directed against MAP-2, GLAST, and the nuclear stain DAPI. The most marked difference was seen in the GLAST staining of the 3/6 DKO cells. Wild-type cells showed a dense network of branched radial processes extending from the neurosphere (Fig. 5A). In 3/6 DKO cells, the processes were flattened and not readily visible (Fig. 5B). The structure of the radial processes in the 1/4/5 TKO cells showed no obvious difference compared to the wild-type cells, if anything, the structure of the radial processes was more clearly distinguishable (Fig. 5C). There were no obvious gross changes in the morphology or density of MAP-2-positive neuronal cells and in the cells from TPRC knockouts (Fig. 5D–F).

The disturbance in the radial glial morphology led us to investigate more closely the neuron-like cells exiting the radial glial layer. A possible way to modulate neuronal cell function is by the direct contact between glial and neuronal cells. The number of neuronal cells, which were separate from or in close contact with radial glial processes, was counted every 2.5 h, during a period of 25 h starting at 20 h of culture. The percentage of free cells was counted at each time point and the data were averaged for each experiment. Figure 6A and B show two classifications: star marked cells are those that are not in contact with radial processes, while arrow-marked cells display the contact point with the radial glial processes. The number of free cells were significantly higher in 3/6 DKO cells than in the WT counterparts (WT $17.5 \pm 3.8\%$ vs. 3/6 DKO $30.4 \pm 6.5\%$, $p < 0.001$) (Fig. 6C; see Online Supplementary Video S1).

To further support the observed change in 3/6 DKO radial glial morphology, we additionally analyzed the radial glial processes by measuring their length (taken from the edge of the neurosphere to the tip of the radial glial processes) using phase-contrast images. As seen in Fig. 6D, a significant difference in glial process lengths was measured between WT and 3/6 DKO (WT: 147.7 ± 43 μm vs. 3/6 DKO: 74.2 ± 26 μm, $p < 0.001$).

Disrupting TRPC3 function significantly increases the distance of migrating cells to radial processes

There are a significant amount of data suggesting that factors produced by radial glia modulate neuronal migration, direct axons, and control synaptogenesis (reviewed in ref. [34]). Therefore, it was of interest to find out whether the distance to radial processes influences the motility pattern of the cells. Thus, the distance of each cell to the nearest radial

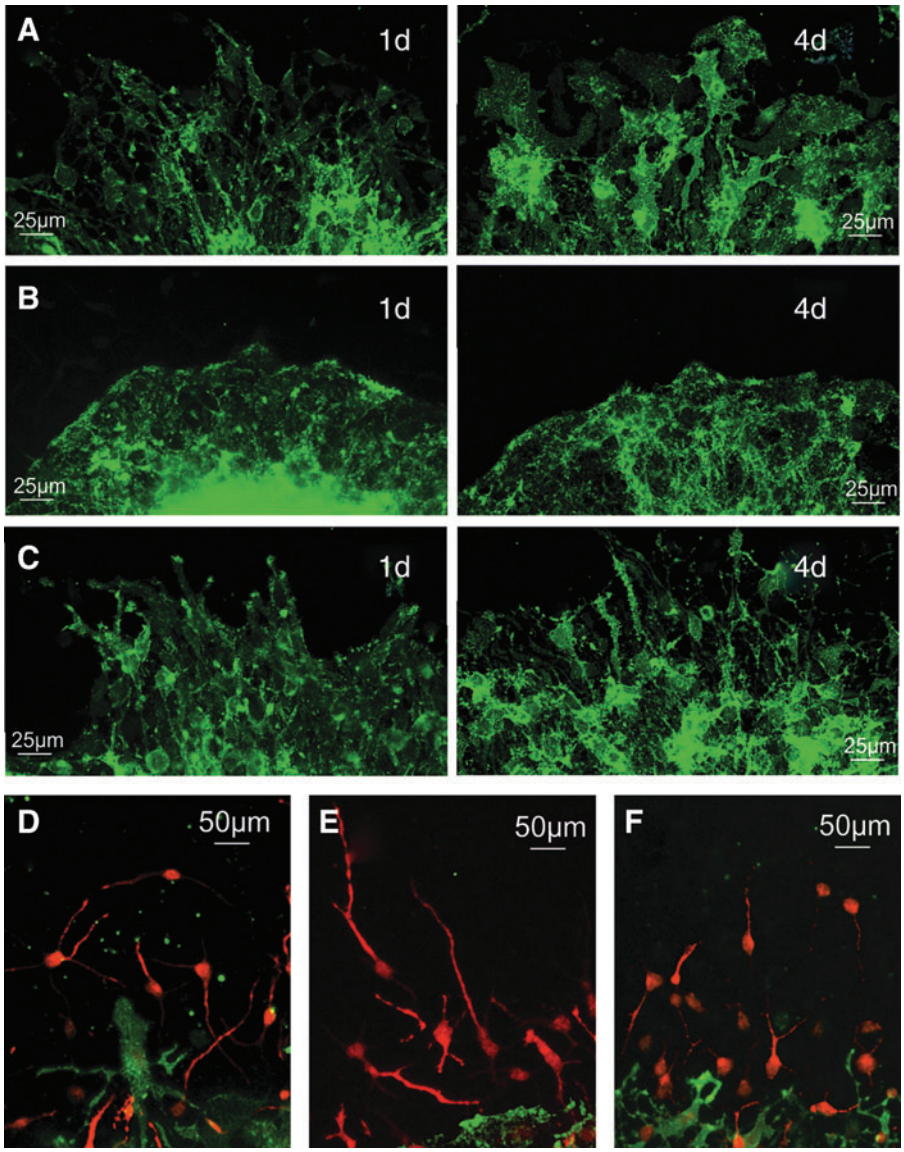

FIG. 5. Effect of 3/6 DKO and 1/4/5 TKO on radial glial structure and the interaction of neuronal cells with radial processes. Wild-type cells stained for glutamate-aspartate transporter (GLAST) at 1 and 4 days of differentiation **(A)**, 3/6 DKO cells stained for GLAST at 1 and 4 days of differentiation **(B)**, and 1/4/5 TKO cells stained for GLAST at 1 and 4 days of differentiation **(C)**. Microtubule-associated protein (MAP-2, *red*) and GLAST (*green*) staining for wild-type cells **(D)**, 3/6 DKO **(E)**, and 1/4/5 TKO **(F)**.

process was analyzed in parallel with the speed of movement. A control cell is shown in Fig. 7A. The stalling periods are marked by arrows. Note that several stalling periods occurred when the cell was very close to the nearest radial process (Fig. 7A, open circles). The pyr3-treated cell in Fig. 7B, however, very seldom stalled close to a radial process. The average distance of the moving cells to radial processes was significantly longer for pyr3-treated cells, MPEP-treated cells, and 3/6 DKO cells compared to control cells (Fig. 6C).

Interestingly, the 1/4/5 TKO cells moved very close to radial processes in a similar way as control cells (see Online Supplementary Video S1). The difference was more marked if the distance to the nearest radial process was measured during the three first stalling periods (Fig. 7D). Again, control and the 1/4/5 TKO cells were on average very close to the radial processes during stalling, while pyr3- and MPEP-treated cells, as well as 3/6 DKO cells stalled much further away from the radial processes (see Online Supplementary Video S1). To analyze further the effect of radial processes on stalling, we plotted the fraction of all cells moving with a speed < 40 μm/h as a function of their distance to the nearest radial processes. As shown in Fig. 7E, the stalling control cells accumulated at a distance of 20 μm from the radial processes, while the distribution of frequency count for pyr3-treated cells (Fig. 7F) and 3/6 DKO cells was broad over a wide range of longer distances. The 1/4/5 TKO cells showed a distribution more similar to the control cells.

Discussion

These results provide a mechanism for the regulation of neuronal progenitor cell migratory behavior and the interaction with external cues mediated by radial glial cells. Our results suggest that the molecular mechanism involves the TRPC3 channel. We further propose that the absence of the functional TPRC3 channel pore leads to migratory disturbances that are dependent on sodium influx and/or local changes to calcium in close proximity to the TRPC channel, in contrast to global changes to intracellular free calcium concentrations. The results of the present study show that (1) TRPC channels are involved in glutamate-evoked G protein-coupled receptor calcium signaling in GLAST-positive

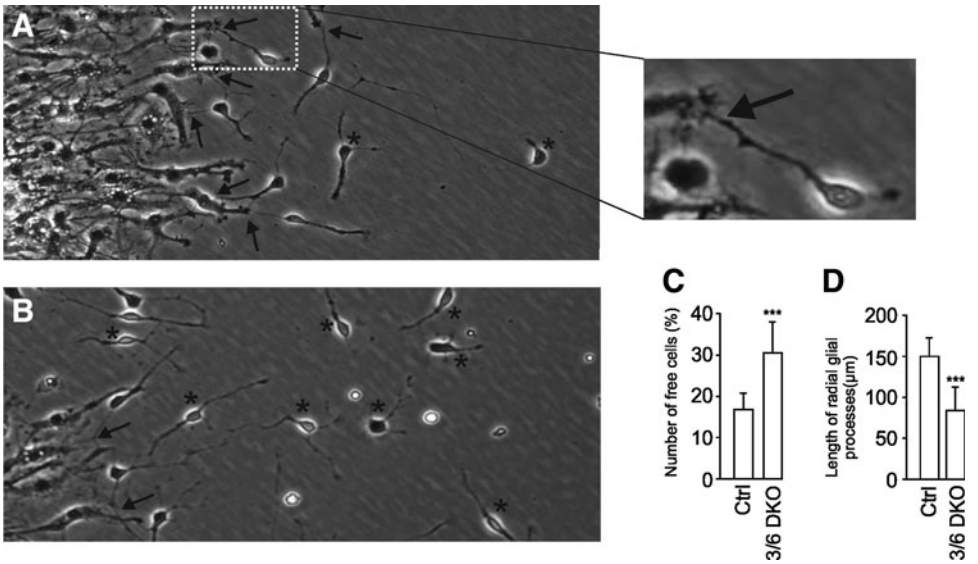

FIG. 6. An image of wild-type cells 36 h after initiation of differentiation **(A)** and an image of 3/6 DKO cells **(B)**. Contact points between thick radial glial processes and thin neuronal processes are shown by *arrows* and unconnected neuronal cells with *stars*. The number of all neuronal cells and neuronal cells that were unconnected or free were counted every 2.5 h during a period of 25 h starting at 20 h of culture. The percentage of free cells at each time point was calculated, and the data were averaged for each experiment. The average of the data from 10 neurospheres is shown ± SD **(C)**. The length of the radial glial processes at 50 h as measured from the edge of each neurosphere to the tip of the process **(D)**. Three to four measurements were performed from each neurosphere and averaged. The data are from four different batches of cells. In each experiment, 8–10 neurospheres were analyzed and averaged. Average ± SD. $***P < 0.001$.

embryonically derived NPCs. (2) TRPC3 is involved in a BDNF-evoked increase in the motility of migration. (3) TRPC3 signaling plays a significant role in the cross talk between radial glial cells and neuronal cells, which dictates the migratory behavior of progenitors with a neuronal fate.

During early development, radial glial cells form supportive frameworks for the migration of neuronal cells to their correct layers in the neocortex. Newborn excitatory neurons migrate from their birthplace to their final laminar position in the cortical plate in close association with radial fibers [35–37]. Additionally, tangentially moving neurons have been shown to form contact points between their leading process and radial glial cells [38]. These observations suggest that radial glial cells are not simply passive tracks for cell migration, but rather actively engage in neuronal–glial signaling that guides neuronal behavior (reviewed in ref. [34]). Despite the clear role of interaction between both cell types, the molecular mechanisms involved are not well investigated.

The neurosphere model offers a possibility to study motility patterns of migrating cells as well as detailed characterization of their functional properties using imaging techniques. Induction of differentiation leads to a migration of cells from the sphere, with radial glial cells residing close to the neurosphere (the inner layers), and an accumulation of maturing neurons at the outer migration layers (reviewed in ref. [39]). Our results show that during the early phases of migration of neurosphere-derived cells, a high *Trpc1* and *Trpc3* mRNA expression was observed. A previous study on *Trpc* mRNA expression at E13 in the embryonic cortex showed the expression of all the *Trpcs* (*Trpc1/3* and *5*) with low expression of *Trpc4/6/7* [40]. In cultured adult hippocampal NPCs, *Trpc1* and *Trpc3–7* were expressed, although *Trpc5* and *Trpc7* were barely detectable [12]. TRPC1 and TRPC3 have been previously shown to be involved in the differentiation of hippocampal neurons [41], guiding growth cones [3,4] and synaptogenesis [42]. Several pieces of evidence have suggested that the subtypes TRPC3/6/7 and TRPC1/4/5 form distinct channel complexes [43]. However, some data implicate that in embryonic brain also TRPC1/3 complexes may exist [9]. A study on the immunocytochemical distribution of TRPC1 and 3 channel expression in embryonic brain demonstrated that while TRPC1 was found exclusively in postmitotic neurons, TRPC3 was found in non-neural cells and precursors [40].

The Ca^{2+} response to DOG, an activator of TRPC3/6/7 channels, and inhibition by pyr3 in a large proportion of the cells demonstrate the functionality of the TRPC3 channels. The response to DOG was absent in cells lacking functional TRPC3 channels (3/6 DKO), while a response could still be elicited in cells lacking functional TRPC1/4/5 channels. A further evidence for the functionality of TRPC3 channels in this cell model is the sensitivity of the response of cells from both the FVB or C57 strain to low concentrations of the TRPC channel blocker pyr3, while no response to the blocker was obtained in the 3/6 DKO cells.

Our data indicate that TRPC1 and TRPC3 channels are involved in the regulation of the phasic motility pattern of neuronal cells. The neuron-like cells showed a distinct phasic pattern of movement, with bursts of linear progression and intermittent slow motility (stalling). During stalling, the typical bipolar morphology of the cells changes to multipolar as they extend processes in many directions. The cells are not totally immobile but rotate with a low speed (below 40 µm/h) and extend processes resulting in typical clusters of movement seen in the spatial motility pattern. Previous studies on developing *xenopus* neurons suggest that during stalling periods, the cells explore the

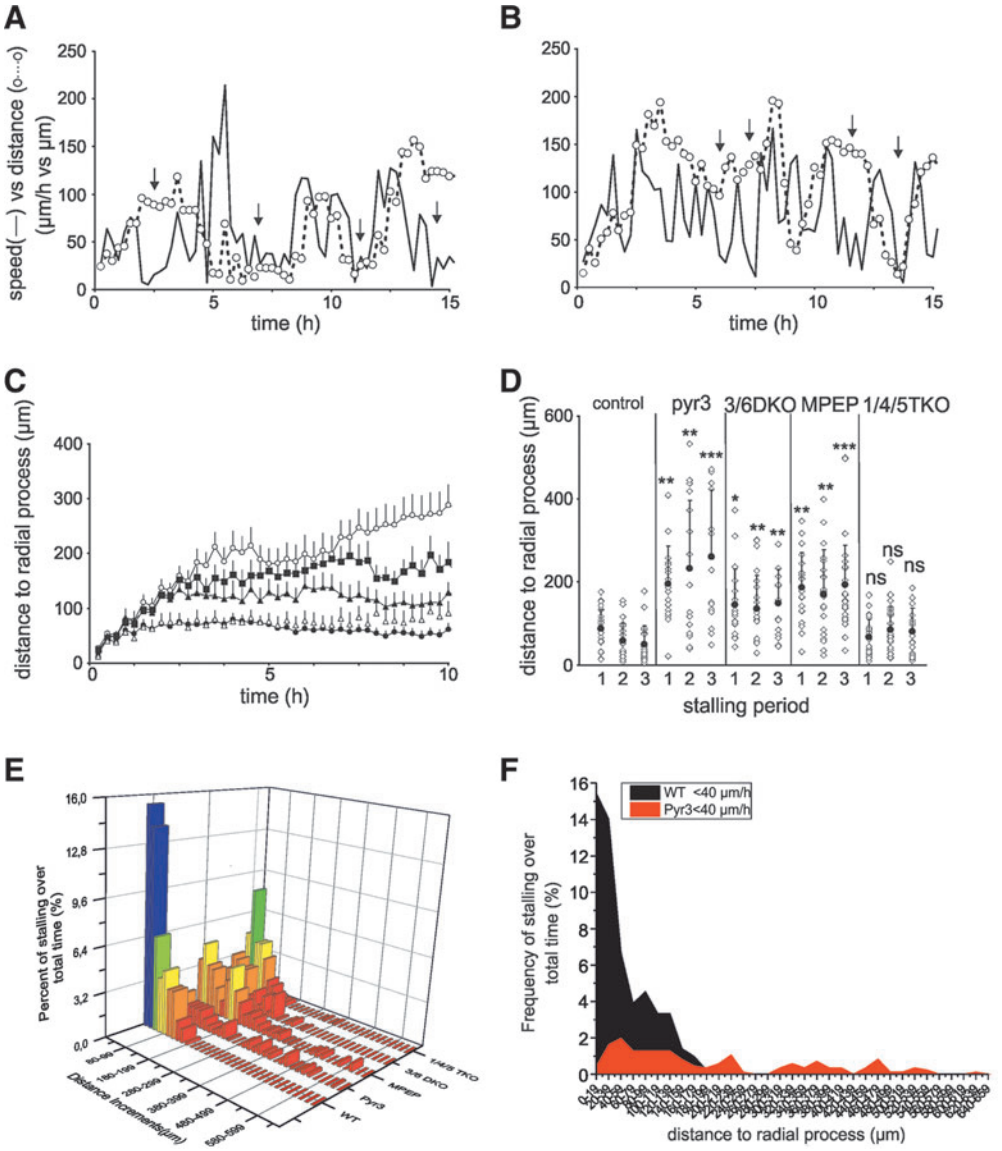

FIG. 7. Correlation between speed and distance to the nearest radial process. **(A)** The speed (*solid line*) of a control cell (C57) and the distance (—○—) to the nearest radial glial process plotted as a function of time. *Arrows* show periods of stalling. **(B)** A cell treated with 1 μM pyr3. **(C, D)** Statistics for experiments similar to **(A, B)**. Cells tracked had to move with a speed above 60 μm/h at least twice or more during a period 10 h or more. In addition, each cell needed to have at least 500 μm free space to move without other neurospheres. **(C)** The distance to the nearest radial process as a function of time for control cells ($N=23$, •), pyr3-treated cells ($N=18$, o), 3/6 DKO cells ($N=20$, ▲), 1/4/5 TKO cells ($N=17$, △), and MPEP-treated cells ($N=21$, ■). **(D)** The distance to the nearest radial glial process during the initial periods of stalling (speed < 40 μm/h). Average ± SD. **(E)** A three-dimensional bar graph plotting frequency count of stalling cells as percentage of total time points (*Z* axis) versus distance from radial glial processes (*Y* axis) in 20 μm increments, for controls, pyr3, MPEP, 3/6 DKO, and 1/4/5 TKO cells (*X* axis). The stalling control cells accumulated at a distance of 20 μm from the radial processes, while the distribution of frequency count for pyr3-treated and 3/6 DKO cells was broad over a wide range of longer distances. The 1/4/5 TKO cells showed a distribution more similar to the control cells. **(F)** An area plot diagram of the same data in **(E)** of WT versus pyr3 showing the distribution profile of the distance increments of the stalling cells. ns, not significant; $*P<0.05$; $**P<0.01$; $***P<0.001$.

environment [44]. The intensity of Ca^{2+} transients increases notably during phases of stalling [44,45]. Also, guidance cues, which induce stalling, cause robust Ca^{2+} elevations [44]. Surprisingly, pyr3-treated cells and 3/6 DKO, as well as 1/4/5 TKO cells all showed an increased motility index (length of phases of high motility divided by length of low motility periods). Since the length of motility bursts was considerably enhanced in cells lacking functional TRPC1 and TRPC3 channels, it is suggested that active channels promote stalling. The expression of TRPC1 is mainly in postmitotic neurons [40]. It thus appears likely that the effect of lack of functional TRPC1 channels directly affects mechanisms controlling the motility of neurons. Interference with TRPC1 function has previously been shown to increase the motility of migrating gonadotropin-releasing hormone (GnRH) neurons [46,47] and the response of growth cones

to guiding cues [3,14]. The mechanism for the increase in motility by interference with TRPC1 channels is probably due to the ability of TRPC1 to interfere with the function of other channel complexes, including those of TRPC3 [47].

The effect of interference with the function of TRPC3 appears complex since the BDNF-promoted increase in the motility index of the neuronal cells was reduced, while the basal motility was increased. BDNF, which promotes neuronal migration [32] and increases the motility index in progenitors [23], has previously been shown to activate TRPC3 channels, which mediate BDNF-induced chemotaxis [4–6]. The lack of an effect of BDNF on the cell motility in the 3/6 DKO cells would thus suggest that TRPC3 channels are also involved in BDNF-promoted motility.

The increased basal motility seen in the absence of functional TRPC3 is most likely due to a different type of mechanism. More detailed analysis of the motility pattern indicated that the effect of lack of TRPC1 and TRPC3 is quite different. Although the 1/4/5 TKO cells showed a higher motility than their wild-type counterparts, they changed direction of movement with about the same frequency, while 3/6 DKO and pyr3-treated cells turned much less. In this respect, cells lacking functional TRPC1 behaved in a way similar to the BDNF-treated cells, which showed a turning frequency similar to the wild-type cells. Since TRPC3 channels appeared to show expression not only in neurons (BDNF response) but also in radial glial cells (response via mGluR5), one possibility would be that radial glial TRPC3 is involved in chemotactic influences that would reduce the motility of neuronal cells.

It has previously been shown that neuronal cells attach to and detach from radial processes [38,48] and that radial glial cells influence the migration of neurons (reviewed in ref. [34]). It is therefore of interest that the neuron-like cells frequently made close contact with radial glial processes and that stalling periods coincided with these interactions. Lack of functional TRPC3 significantly reduced these interactions and the cells tended to avoid the radial glial processes. Lack of attracting cues from radial glial processes would also explain the reduction in turning frequency in response to inhibition/lack of TRPC3 function.

The motility pattern seen with lack of TRPC3 with a high motility index, low turning frequency, and lack of radial process interaction is reminiscent of the effect of MPEP, a blocker of mGluR5, which shows a similar motility pattern [20]. Several factors point to a role of the mGluR5/TRPC3 pair in the interaction between radial glia and the neuronal cells. The mGluR5 receptor appears to be expressed almost exclusively in radial glial cell-based distribution of calcium response to the agonist DHPG, an agonist of mGluR5, and immunostaining for mGluR5. The inner migration layer of embryonic cortical neurosphere-derived cells containing radial glia shows robust responses and immunostaining, while no signal is obtained in the outer layer containing mainly MAP-2 immunoreactive neuronal cells [20,49]. The above mentioned i) mGluR5 cell layer distribution ii) the similarity of the effects on the motility response by blocking with MPEP and interfering with TRPC3 channel function iii) block of the DHPG induced Ca^{2+} influx by pyr3 and iv) that both interference of TRPC3 function (this study) and MPEP distort the structure of radial processes [20,49], would suggest that mGluR5 acting via TRPC3 is part of a communication pathway between radial glial and neuronal cells.

Coupling of group I metabotropic glutamate receptors (mGluR1 and 5) to TRPC3 channels has been shown earlier in postnatal neurons [15]. Even if pyr3 blocked the Ca^{2+} response to DHPG, indicating coupling to TRPC3, there was no measurable difference in the global Ca^{2+} response to DHPG in the 3/6 DKO cells. It is likely that in our case, compensatory mechanisms are involved. Such mechanisms, however, do not appear to compensate for the mechanisms required for neuronal motility. This is in line with previous studies in postnatal Purkinje cells [50] that showed that the calcium response to DHPG was not altered in TRPC3-deficient cells, while synaptic currents are considerably altered. Taken together, our data suggest that even if the neuronal cells whose motility was analyzed appear to move freely, their motility is constantly modulated by factors secreted from the radial glial processes.

Information concerning the role of mGluR5/TRPC3 in brain development in vivo is limited. The studies done on TRPC3 and mGluR5 knockouts report no marcoanatomical anomalies in either the cortical or granular layer organization. mGluR5 knockout studies point toward alterations in cell segregation in specific areas of cortical layer IV as well as in dendritic spine morphology and density [51,52]. These studies highlight the role that mGluR5 receptors play in potentially influencing synaptic function in the brain. TRPC3 knockout animals have demonstrated that TRPC3 is required for both normal motor behavior and normal synaptic function in cerebellar Purkinje cells [50]. Furthermore, in a TRPC3-deficit mouse model, in which the promoter region of TRPC3 is disrupted, there is an abnormal expansion of astrocytes in the white matter of the brain, cerebellum, and spinal cord and progressive degeneration along with necrosis of spinal motor neurons, which develops to a progressive paralysis of the hind limbs [53,54]. Our in vitro finding that the interaction between glial cells and neuronal progenitor cells is impaired leading to changes in cell motility when TRPC3/mGluR5 channels are blocked with alterations in the calcium signaling brought about through mGluR5 may perpetuate itself in synaptic function. Impairing TRPC/mGluR5 function reduced contact-based signaling between the progenitor cells and the radial glial network.

In conclusion, our data suggest that TRPC1 and TRPC3 channels play an important role in regulating the motility of NPCs in vitro. TRPC1 interference with its function leads to an increase in cell motility. In neurons, TRPC3 channels are involved in BDNF-induced increase in motility. mGluR5 acting through TRPC3 channels seems to have a central role in the communication between radial glia and neuronal cells.

Acknowledgments

The authors would like to thank Mr. Jarno Hörhä and Mr. Matti-Pekka Poikajärvi for their laboratory assistance. They are also very grateful for receiving the transgenic mice and manuscript comments by Prof. Veit Flockerzi, Prof. Marc Freichel, Prof. Lutz Birnbaumer, and Dr. Andreas Beck. This study was supported by the Academy of Finland, the Finnish Medical Society, the Magnus Ehrnrooth Foundation, the Swedish Cultural Foundation in Finland, Medicinska Understödsföreningen Liv och Hälsa r.f., the University of Helsinki Funds.

Author Disclosure Statement

The authors indicate no potential conflicts of interest.

References

1. Rakic P, AE Ayoub, JJ Breunig and MH Dominguez. (2009). Decision by division: making cortical maps. Trends Neurosci 32:291–301.
2. Wang GX and MM Poo. (2005). Requirement of TRPC channels in netrin-1-induced chemotropic turning of nerve growth cones. Nature 434:898–904.
3. Shim S, EL Goh, S Ge, K Sailor, JP Yuan, HL Roderick, MD Bootman, PF Worley, H Song and GL Ming. (2005). XTRPC1-dependent chemotropic guidance of neuronal growth cones. Nat Neurosci 8:730–735.
4. Li Y, YC Jia, K Cui, N Li, ZY Zheng, YZ Wang and XB Yuan. (2005). Essential role of TRPC channels in the guidance of nerve growth cones by brain-derived neurotrophic factor. Nature 434:894–898.
5. Li HS, XZ Xu and C Montell. (1999). Activation of a TRPC3-dependent cation current through the neurotrophin BDNF. Neuron 24:261–273.
6. Amaral MD and L Pozzo-Miller. (2007). BDNF induces calcium elevations associated with IBDNF, a nonselective cationic current mediated by TRPC channels. J Neurophysiol 98:2476–2482.
7. Louhivuori V, A Vicario, M Uutela, T Rantamaki, LM Louhivuori, E Castren, E Tongiorgi, KE Akerman and ML Castren. (2011). BDNF and TrkB in neuronal differentiation of Fmr1-knockout mouse. Neurobiol Dis 41:469–480.
8. Riccio A, AD Medhurst, C Mattei, RE Kelsell, AR Calver, AD Randall, CD Benham and MN Pangalos. (2002). mRNA distribution analysis of human TRPC family in CNS and peripheral tissues. Brain Res Mol Brain Res 109:95–104.
9. Strubing C, G Krapivinsky, L Krapivinsky and DE Clapham. (2003). Formation of novel TRPC channels by complex subunit interactions in embryonic brain. J Biol Chem 278:39014–39019.
10. Fiorio Pla A, D Maric, SC Brazer, P Giacobini, X Liu, YH Chang, IS Ambudkar and JL Barker. (2005). Canonical transient receptor potential 1 plays a role in basic fibroblast growth factor (bFGF)/FGF receptor-1-induced Ca2+ entry and embryonic rat neural stem cell proliferation. J Neurosci 25:2687–2701.
11. Weick JP, M Austin Johnson and SC Zhang. (2009). Developmental regulation of human embryonic stem cell-derived neurons by calcium entry via transient receptor potential channels. Stem Cells 27:2906–2916.
12. Li M, C Chen, Z Zhou, S Xu and Z Yu. (2012). A TRPC1-mediated increase in store-operated Ca2+ entry is required for the proliferation of adult hippocampal neural progenitor cells. Cell Calcium 51:486–496.
13. Paez PM, D Fulton, V Spreuer, V Handley and AT Campagnoni. (2011). Modulation of canonical transient receptor potential channel 1 in the proliferation of oligodendrocyte precursor cells by the golli products of the myelin basic protein gene. J Neurosci 31:3625–3637.
14. Kim SJ, YS Kim, JP Yuan, RS Petralia, PF Worley and DJ Linden. (2003). Activation of the TRPC1 cation channel by metabotropic glutamate receptor mGluR1. Nature 426: 285–291.
15. Berg AP, N Sen and DA Bayliss. (2007). TrpC3/C7 and Slo2.1 are molecular targets for metabotropic glutamate receptor signaling in rat striatal cholinergic interneurons. J Neurosci 27:8845–8856.
16. Di Giorgi Gerevini VD, A Caruso, I Cappuccio, L Ricci Vitiani, S Romeo, C Della Rocca, R Gradini, D Melchiorri and F Nicoletti. (2004). The mGlu5 metabotropic glutamate receptor is expressed in zones of active neurogenesis of the embryonic and postnatal brain. Brain Res Dev Brain Res 150:17–22.
17. Baskys A, I Bayazitov, L Fang, M Blaabjerg, FR Poulsen and J Zimmer. (2005). Group I metabotropic glutamate receptors reduce excitotoxic injury and may facilitate neurogenesis. Neuropharmacology 49 Suppl 1:146–156.
18. Simonyi A, TR Schachtman and GR Christoffersen. (2005). The role of metabotropic glutamate receptor 5 in learning and memory processes. Drug News Perspect 18:353–361.
19. Gandhi R, KC Luk, VV Rymar and AF Sadikot. (2008). Group I mGluR5 metabotropic glutamate receptors regulate proliferation of neuronal progenitors in specific forebrain developmental domains. J Neurochem 104:155–172.
20. Jansson LC, L Louhivuori, HK Wigren, T Nordstrom, V Louhivuori, ML Castren and KE Akerman. (2013). Effect of glutamate receptor antagonists on migrating neural progenitor cells. Eur J Neurosci 37:1369–1382.
21. Castren M, T Tervonen, V Karkkainen, S Heinonen, E Castren, K Larsson, CE Bakker, BA Oostra and K Akerman. (2005). Altered differentiation of neural stem cells in fragile X syndrome. Proc Natl Acad Sci U S A 102:17834–17839.
22. Karkkainen V, V Louhivuori, ML Castren and KE Akerman. (2009). Neurotransmitter responsiveness during early maturation of neural progenitor cells. Differentiation 77: 188–198.
23. Jansson LC, L Louhivuori, HK Wigren, T Nordstrom, V Louhivuori, ML Castren and KE Akerman. (2012). Brain-derived neurotrophic factor increases the motility of a particular N-methyl-D-aspartate/GABA-responsive subset of neural progenitor cells. Neuroscience 224:223–234.
24. Stroh O, M Freichel, O Kretz, L Birnbaumer, J Hartmann and V Egger. (2012). NMDA receptor-dependent synaptic activation of TRPC channels in olfactory bulb granule cells. J Neurosci 32:5737–5746.
25. Quick K, J Zhao, N Eijkelkamp, JE Linley, F Rugiero, JJ Cox, R Raouf, M Gringhuis, JE Sexton, et al. (2012). TRPC3 and TRPC6 are essential for normal mechanotransduction in subsets of sensory neurons and cochlear hair cells. Open Biol 2:120068.
26. Louhivuori LM, V Louhivuori, HK Wigren, E Hakala, LC Jansson, T Nordstrom, ML Castren and KE Akerman. (2013). Role of low voltage activated calcium channels in neuritogenesis and active migration of embryonic neural progenitor cells. Stem Cells Dev 22:1206–1219.
27. Elg S, F Marmigere, JP Mattsson and P Ernfors. (2007). Cellular subtype distribution and developmental regulation of TRPC channel members in the mouse dorsal root ganglion. J Comp Neurol 503:35–46.
28. Tai Y, S Feng, W Du and Y Wang. (2009). Functional roles of TRPC channels in the developing brain. Pflugers Arch 458:283–289.
29. Murase S and AF Horwitz. (2002). Deleted in colorectal carcinoma and differentially expressed integrins mediate the directional migration of neural precursors in the rostral migratory stream. J Neurosci 22:3568–3579.
30. Suzuki SO and JE Goldman. (2003). Multiple cell populations in the early postnatal subventricular zone take distinct

migratory pathways: a dynamic study of glial and neuronal progenitor migration. J Neurosci 23:4240–4250.
31. Ward ME, H Jiang and Y Rao. (2005). Regulated formation and selection of neuronal processes underlie directional guidance of neuronal migration. Mol Cell Neurosci 30:378–387.
32. Dicou E. (2009). Neurotrophins and neuronal migration in the developing rodent brain. Brain Res Rev 60:408–417.
33. Rae MG and AJ Irving. (2004). Both mGluR1 and mGluR5 mediate Ca2+release and inward currents in hippocampal CA1 pyramidal neurons. Neuropharmacology 46:1057–1069.
34. Sild M and ES Ruthazer. (2011). Radial glia: progenitor, pathway, and partner. Neuroscientist 17:288–302.
35. Rakic P. (1971). Neuron-glia relationship during granule cell migration in developing cerebellar cortex. A Golgi and electronmicroscopic study in *Macacus rhesus*. J Comp Neurol 141:283–312.
36. Rakic P. (1972). Mode of cell migration to the superficial layers of fetal monkey neocortex. J Comp Neurol 145:61–83.
37. Rakic P. (1988). Specification of cerebral cortical areas. Science 241:170–176.
38. O'Rourke NA, DP Sullivan, CE Kaznowski, AA Jacobs and SK McConnell. (1995). Tangential migration of neurons in the developing cerebral cortex. Development 121:2165–2176.
39. Ahmed S. (2009). The culture of neural stem cells. J Cell Biochem 106:1–6.
40. Boisseau S, C Kunert-Keil, S Lucke and A Bouron. (2009). Heterogeneous distribution of TRPC proteins in the embryonic cortex. Histochem Cell Biol 131:355–363.
41. Wu X, TK Zagranichnaya, GT Gurda, EM Eves and ML Villereal. (2004). A TRPC1/TRPC3-mediated increase in store-operated calcium entry is required for differentiation of H19-7 hippocampal neuronal cells. J Biol Chem 279:43392–43402.
42. Zhou J, W Du, K Zhou, Y Tai, H Yao, Y Jia, Y Ding and Y Wang. (2008). Critical role of TRPC6 channels in the formation of excitatory synapses. Nat Neurosci 11:741–743.
43. Hofmann T, M Schaefer, G Schultz and T Gudermann. (2002). Subunit composition of mammalian transient receptor potential channels in living cells. Proc Natl Acad Sci U S A 99:7461–7466.
44. Gomez TM and NC Spitzer. (1999). In vivo regulation of axon extension and pathfinding by growth-cone calcium transients. Nature 397:350–355.
45. Gomez TM and NC Spitzer. (2000). Regulation of growth cone behavior by calcium: new dynamics to earlier perspectives. J Neurobiol 44:174–183.
46. Ariano P, S Dalmazzo, G Owsianik, B Nilius and D Lovisolo. (2011). TRPC channels are involved in calcium-dependent migration and proliferation in immortalized GnRH neurons. Cell Calcium 49:387–394.
47. Storch U, AL Forst, M Philipp, T Gudermann and M Mederos y Schnitzler. (2012). Transient receptor potential channel 1 (TRPC1) reduces calcium permeability in heteromeric channel complexes. J Biol Chem 287:3530–3540.
48. O'Rourke NA, ME Dailey, SJ Smith and SK McConnell. (1992). Diverse migratory pathways in the developing cerebral cortex. Science 258:299–302.
49. Jansson LC and KE Akerman. (2014). The role of glutamate and its receptors in the proliferation, migration, differentiation and survival of neural progenitor cells. J Neural Transm 121:819–836.
50. Hartmann J, E Dragicevic, H Adelsberger, HA Henning, M Sumser, J Abramowitz, R Blum, A Dietrich, M Freichel, et al. (2008). TRPC3 channels are required for synaptic transmission and motor coordination. Neuron 59:392–398.
51. Wijetunge LS, SM Till, TH Gillingwater, CA Ingham and PC Kind. (2008). mGluR5 regulates glutamate-dependent development of the mouse somatosensory cortex. J Neurosci 28:13028–13037.
52. Chen CC, HC Lu and JC Brumberg. (2012). mGluR5 knockout mice display increased dendritic spine densities. Neurosci Lett 524:65–68.
53. Rodriguez-Santiago M, M Mendoza-Torres, JF Jimenez-Bremont and R Lopez-Revilla. (2007). Knockout of the trcp3 gene causes a recessive neuromotor disease in mice. Biochem Biophys Res Commun 360:874–879.
54. Lopez-Revilla R, C Soto-Zarate, C Ridaura, L Chavez-Duenas and D Paul. (2004). Progressive paralysis associated with diffuse astrocyte anaplasia in delta 202 mice homozygous for a transgene encoding the SV40 T antigen. Neuropathology 24:30–37.

Address correspondence to:
Prof. Karl E. Åkerman
Biomedicum Helsinki
Institute of Biomedicine/Physiology
University of Helsinki
P.O. Box 63
Helsinki 00014
Finland

E-mail: karl.akerman@helsinki.fi

Received for publication April 29, 2014
Accepted after revision October 25, 2014
Prepublished on Liebert Instant Online October 27, 2014